Published in final edited form as:

Lab Chip. 2018 April 17; 18(8): 1207–1214. doi:10.1039/C8LC00001H.

3D-printed Quake-style microvalves and micropumps†

Yuan-Sheng Lee[a], **Nirveek Bhattacharjee**[b], **Albert Folch**[b]

[a]Department of Mechanical Engineering, University of Washington, USA.

[b]Department of Bioengineering, University of Washington, USA

Abstract

Here we demonstrate a 3D-printable microvalve that is transparent, built with a biocompatible resin, and has a simple architecture that can be easily scaled up into large arrays. The open-at-rest valve design is derived from Quake's PDMS valve design. We used a stereolithographic (SL) 3D printer to print a thin (25 or 10 μm-thick) membrane (1200 or 500 μm-diam.) that is pneumatically pressed (~3–6 psi) over a bowl-shaped seat to close the valve. We used poly(ethylene diacrylate) (MW = 258) (PEG-DA-258) as the resin because it yields transparent cytocompatible prints. Although the flexibility of PEG-DA-258 is inferior to that of other microvalve fabrication materials such as PDMS, the valve benefits from the bowl design and the membrane's high restoring force since it does not need a negative pressure to re-open. We also 3D-printed a micropump by combining three Quake-style valves in series. The micropump only requires positive pressure for its operation and profits from the fast return to the valves' open states. Moreover, we printed a 64-valve array constructed with 500 μm-diam. valves to demonstrate the reliability and scalability of the valves. Overall, we demonstrate the 3D-printing of compact microvalves and micropumps using a process that precludes the need for specialized, time-consuming labor.

Introduction

Microvalves and micropumps are fundamental components of many microfluidic systems.[1–8] Using microvalves, temporal sequences of fluids can be programmed to produce combinatorial mixtures and gradients,[9–13] droplet combinations,[14] nucleic acid manipulations,[15–17] and cell culture conditions.[18,19] Additionally, microvalves allow for tuning of flow resistance[20] and microchannel topography[21] (among other operations) at a spatiotemporal scale that is inaccessible to manual manipulation. Microfluidic automation spares the costs of human labor and enables faster processing through miniaturization and parallelization.[6,22,23]

The Quake group first introduced normally-open valves with a very simple three-layer architecture made in poly(dimethyl siloxane) (PDMS): a microchannel lying orthogonally

†Electronic supplementary information (ESI) available. See DOI: 10.1039/c8lc00001h

ysleetw@uw.edu.

Conflicts of interest

There are no conflicts to declare.

on top of another microchannel with a thin elastomeric membrane in between[2] (Fig. 1a). One of the micro-channels acts as a "control channel" that, when pressurized, causes deflection of the membrane to interrupt the flow in the orthogonal "flow channel". Quake valves have found many applications because their design and working principle are extremely simple. Most research groups that produce Quake valves make them in PDMS from photolithographically-fabricated molds. However, the commercial ordering of photo-masks, followed by photolithography and PDMS molding, is a process that typically consumes several days. Even if the photo-mask step is expedited by an internal service, photolithography and PDMS molding are processes that take several hours each. Moreover, stacking multiple PDMS layers to create 3D micro-channels requires tedious manual labor and delicate, operator-dependent craftsmanship for aligning and bonding (*i.e.* Quake valves have to be made by skilled personnel); importantly, these manual processes can have an impact on manufacturing yield and device quality.

3D-printing offers an alternative to manual processing. 3D-printed micro-components such as microchannels,[24–28] microvalves, and micropumps[24,29,30] have become important and are widely used in the field of microfluidics owing to their compact size, easy and rapid manufacturing, and high integration ability.[31,32] One of the first 3D-printed valves was SL-printed using the commercial resin Watershed and enabled the possibility of building microfluidic perfusion systems compatible with cells.[24] Due to resolution limitations, Watershed microvalves and micropumps are much larger than PDMS ones, which leads to large dead volumes and makes the integration with other microfluidic components more difficult. Recently, Nordin *et al.*[33] have demonstrated 3D-printed microvalves ~1 mm in diameter which can be fabricated in a resin made of poly-ethylene glycol diacrylate (MW ~258) (PEG-DA-258) and an orange UV-absorber (Sudan I), demonstrating the suitability of this photopolymerizable resin as a 3D-printable micromechanical material (adding to its biocompatibility demonstrated for 3D-printed microfluidics[34]). However, both our Watershed and Nordin's valve designs have a complex 3D architecture, which presents a few challenges: 1) microscopic observation of the valve operation is difficult due to the valve's 3D architecture; 2) integration of valve arrays requires 3D-piping, and 3) draining of the PEG-DA-258 precursor after printing becomes problematic as the complexity of the valve array grows.

Here we present a modified version of the Quake valve that can be 3D-printed using transparent PEG-DA-258. This modified design, which we term as a "Quake-style" valve, features a bowl-shaped valve seat (*i.e.* the seat is shaped as a hemispherical cap) for improved printability and operation, and offers notable design advantages in terms of microscopy and piping simplicity for future large-scale arrays.

Results and discussion

Unlike photolithography, 3D CAD design allows for optimizing the overall symmetry of the valve seat and, consequently, the sealing ability of the valve. We first printed the original Quake-style valve (Fig. 1a and S1, ESI†), consisting of a rectangular control channel placed on top of a semicircular-cross-section flow channel. However, our resin is composed of PEG-DA-258 (Young's modulus $E \sim 130$ MPa),[35] which is about 130 times less flexible

than PDMS ($E < 1$ MPa).[36] As a result, the deflected PEG-DA-258 membrane (dimensions: 1000 μm × 1000 μm, membrane thickness: 25 μm) cannot seal against the bottom of the flow channel even after applying pressures greater than 10 psi. Although in principle the deflection of the membrane (for any given pressure) could have been increased by expanding its size, we decided to exploit the degree of freedom offered by 3D-printing that photolithographic fabrication does not have. Specifically, using photolithography-based processes, Quake valve channels must have constant cross-sections along the channel axis, while 3D-printing is able to generate channels with variable cross-sections. We designed the seat of the 3D-printed Quake-style valve with a bowl-shaped structure that was elevated with respect to the bottom of the flow channel so that the membrane (diam.: 1200 μm, thickness: 25 μm) could easily reach the valve seat and seal the valve upon deflection at lower control pressures (<10 psi) compared to the original Quake valve design. The curvature of the bowl shape helps create a smooth seal between the membrane and the seat. Furthermore, the flow channel partially overlaps with the valve seat in order to avoid overexposure of uncured resin. Note that this overlap design (a necessary compromise feature) prevents the bowl from being perfectly circular (Fig. S2†). Last but not the least, the two edges of the valve seat, which correspond to the thinnest parts of the flow channel, were ~40 μm below the membrane (Fig. 1b & S2†). The flow channel got clogged during fabrication of the control channel if the gap was smaller than 40 μm (parameter d in Fig. S2†). This design constraint guaranteed that the flow-channel void on top of the valve seat received the least possible dose of additional UV exposure when the additional Z-layers of the control channel walls were printed. The STL files of both two valve designs are available in ESI.†

The architecture and functioning principle of the valve are shown in Fig. 2. The Quake-style microvalve was printed with an Asiga Pico2-HD SL 3D-printer which has a projected XY pixel resolution of 27 μm. We used PEG-DA-258 resin containing 0.6% (w/w) Irgacure-819 as a photoinitiator and 0.6% (w/w) 2-isopropyl thioxanthone (ITX) as a UV photosensitizer. This mixture has been carefully optimized for resolution and biocompatibility.[37] As shown in Fig. 2a & b, the size of the 3D-printed Quake-style valve is around one order of magnitude smaller in diameter than the one that Au *et al.* made in Watershed.[24] The valve devices were printed with 25 μm Z-layer thickness. Other than the bowl-shaped valve seat, our 3D-printed Quake-style valve basically follows the design of the original Quake valve, with a control channel on top of a flow channel (Fig. 2c & d). The membrane layer is printed as a single 25 μm-thick Z layer between the flow channel and the control channel along the Z-axis. The equation describing the relationship between applied pressure P and membrane deflection y at the center of a thin circular membrane of thickness t made of a material of Young's modulus E and Poisson's ratio v is:

$$\frac{Pr^4}{Et^4} = \frac{5.33}{1-v^2} \cdot \frac{y}{t} + \frac{2.6}{1-v^2} \cdot \left(\frac{y}{t}\right)^3 \quad (1)$$

According to eqn (1), a membrane of $r = 0.6$ mm (diam. = 1200 μm) and $E = 130$ MPa deflects by $y = 101.7$ μm at $P = 6$ psi. Considering the Z-layer resolution of the printer (the printer can print in Z increments of 25 μm), we decided to design a bowl with a depth of 100 μm to ensure that the valve could be closed at 6 psi. We note that the depth of the bowl also

determines the vertical gap from the edge of the bowl to the bottom of the membrane (d = 40 μm in Fig. S2, ESI†), which is a critical parameter because gaps lower than 40 μm result in channel clogging when the Z-layer thickness is 25 μm. Hence, although it is possible to print a valve with a bowl depth of 75 μm (which would in principle be preferable because it is predicted to close at 3.92 psi), it does not print well with the present absorptivity of our resin.

The functioning principle of the valve is shown in Fig. 2e and f. For the operation of the valve, the control channel was pressurized with air and the flow channel was filled with blue dye (FD&C blue #1, Spectrum, New Brunswick). When zero pressure is applied to the control channel, the membrane does not deflect and the flow channel remains open; when pressure is applied, the membrane deflects. At 6 psi, the membrane contacts the bottom of the bowl-shaped structure and seals the flow channel. With 6 psi, all valves tested were completely closed without damaging or rupturing the valves. There is only a 1.7% difference of deflection distance (y) between the real membrane deflection and the predicted deflection calculated from eqn (1), showing the printer's reliability. To test the valve's durability, the valve was operated under 6 psi at a frequency of 10 Hz for over 16 hours; within that period, the valve was actuated over 500 000 times. After the 16 hour-long test, the valve could still be closed at 6 psi.

We characterized the fluidic resistance of the valve by measuring the flow rate and electrical current through the valve for a given head pressure (see setup schematic in Fig. 3a). We found that by applying 4 psi to the control channel, the flow rate decreased 10 times (~12 μL min^{-1}) compared to the flow rate when no pressure is applied (~120 μL min^{-1}). However, the flow was not fully stopped until air pressure greater than 5 psi was applied to the control channel (Fig. 3b). Parameters such as machine resolution, vat condition, and resin chemistry could influence the variability in flow rates observed between prints. The more accurate current measurements in Fig. 3c show that the valve does not fully close until the control pressure reaches 6 psi. The detected current value was ~700 mA when there was no control pressure applied to the valve and it went down to a negligible ~4 mA (0.5% of 700 mA) as the control pressure was greater than 6 psi. Idealizing the valve as a circular pipe of diameter D, the current is roughly proportional to D^2, and the fluidic resistance of the pipe is proportional to $1/D^2$, so a closed-valve current value of 0.5% = 1/200 of the open-valve current value implies a closed-state fluidic resistance that is ~200 times higher than the open-state fluidic resistance. It is important to keep in mind that the membrane deflection is determined by the pressure difference between the control channel and the flow channel. Thus, applying high driving pressure in the flow channel can prevent the valve from closing and even damage the membrane.

Next, we characterized the dynamic behavior of the valve by measuring the current that passes through a saline-filled flow channel while the valve is being actuated at different frequencies. The device setup is shown in Fig. 4a. A high current amplitude represents the valve open state and a low current amplitude represents the valve closed state. At 5 Hz, the valve was able to open and close as described by the high peak-to-peak current amplitude compared to higher frequencies of 20 and 30 Hz. At these high frequencies, the peak-to-peak current amplitude decreased, signifying that the valve was no longer able to fully open

or fully close. At 5 Hz, the valve remained open for ~100 ms during a full cycle of opening and closing, shown by a plateau after the rising phase of the electrical current curve (Fig. 4b, black arrow). The valve took approximately 100 ms to close, of which it spent ~20 ms fully closed (Fig. 4b, white arrow). As the frequency was increased, the time period of the plateaus became shorter, meaning the valve's reaction time was not fast enough to react to the even faster changes in air pressure signal in the control channel (Fig. 4b, dashed black line). A movie of the valve actuation at different frequencies is shown in ESI† (Movie S1).

Integrated micropumps add portability and reduce the number of external accessories in microfluidic chips.[38–40] Our 3D-printed Quake-style pumps were made by combining three valves in series (Fig. 5). A smaller valve leads to a membrane with a faster reaction time and higher resonance frequency, thereby propelling fluid more efficiently. While the higher stiffness of PEG-DA-258 compared to PDMS is a disadvantage during the deflection phase, it provides a high restoring force for the membrane to quickly return to its resting position without the application of negative pressure. The STL file of the micropump design is available in ESI.†

The pump was operated by following a standard peristaltic sequence (shown in Fig. 6a). In this sequence, there are 5 states and the switching period (T) between each state ranges from 10 ms to 500 ms. Here, pump actuation frequency (f) is defined as $1/T$. Even though the valves were opened and closed almost completely with low pump actuation frequencies, the fluid movement was too slow to be observed at 5 Hz (Movie S2, ESI†). With a fixed control pressure of 7 psi, the flow rate reached a maximum of ~6.5 μL min^{-1} at a pump actuation frequency of 20 Hz (Fig. 6b). Although the valves did not fully close and open at a pump actuation frequency of 20 Hz, which is the same frequency at which each valve is actuated, the rapid opening and closing of the valves still displaced liquid and compensated for the lower pumping efficiency. We calculated that the amount of fluid pumped by each valve in 1 min is 32 nL at 5 Hz and 18 nL at 20 Hz. Despite the fact that the valves pumped around half the volume at 20 Hz compared to 5 Hz, in the same amount of time they opened and closed four times more often at 20 Hz compared to 5 Hz, so in total the pumping rate at 20 Hz (21.6 μL min^{-1}) was about twice the pumping rate at 5 Hz (9.6 μL min^{-1}). We also determined the maximum head pressure that the 3D-printed pump can overcome (maximum pump back pressure). For these experiments we used a control pressure of 14 psi to actuate the pump and the pump actuation frequency was 20 Hz. Under these conditions, the pump was able to overcome at most a head pressure of 0.2 psi, which is equal to the pressure exerted by a 140 mm column of water (Fig. 6c); as the pressure that was applied at the outlet of the flow channel increased above 0.2 psi, the flow started to move backward (represented as negative flow values in Fig. 6c).

One of the powerful features of the Quake design is its scalability. We decided to test the scalability of the Quake-style design by reducing its size to a diameter of 500 μm (membrane thickness 10 μm and bowl depth 75 μm; see Fig. S2†) and by producing three identical arrays of 8 × 8 = 64 valves each. One of the arrays is shown in Fig. 7. Here the control channels have also been reduced to 300 μm width. We were able to print, rinse, and operate all 64 valves in all three arrays. Only 3 psi was needed to close these smaller valves. We also tested the durability of the valve array, which could be actuated at 10 Hz (3 psi of

closing pressure) over 500 000 times. This compact valve array not only demonstrates the scalability of the Quake-style design but also shows the high yield and reliability of the 3D-printing process.

Summary

In conclusion, we have demonstrated a 3D-printable valve based on a simple design concept consisting of two orthogonally-intersecting channels. This design is a modified version of the popular PDMS-based design popularly known as a “Quake valve”, so we dubbed our valve as a “Quake-style valve”. The major design modification of the Quake-style valve is a raised bowl-shaped valve seat that makes the membrane establish contact with the seat more isotropically and at a lower pressure compared to a Quake valve made with the same materials and dimensions. The valve was successfully 3D-printed in a transparent, biocompatible resin[34] and was pneumatically operated by applying a wide range of air pressures (3–10 psi) to the control channel. A pump was also successfully built by combining 3 valves in series. We were able to propel fluid in the channel by controlling the opening and closing of each valve. Integrated microfluidic 3D-printed valves and pumps are designed by using 3D-modeling software, assembled into a single 3D-design file and fabricated in a single print. This process helps accelerate the prototyping phase by facilitating trial-and-error and online collaborations.

We anticipate that the mechanical performance and the packing density of the valves will improve as the resolution of the printers improve in the near future and as new resins with low Young’s modulus and high molar UV absorptivity become available. A number of elastomeric resins are already available but they are either not transparent or not biocompatible, so efforts in resin photochemistry and improved printers will be essential in the development of future microactuators. We believe that digital manufacturing methods such as stereolithography will substantially lower the cost of microfluidic devices and streamline their complex fabrication process.

Methods

Materials for 3D printing

We use poly(ethylene glycol) diacrylate (MW = 258) (PEG-DA-258, Sigma-Aldrich, MO), mixed with 0.6% (w/w) Irgacure-819 (photoinitiator) (BASF, IL) and 0.6% (w/w) 2-isopropyl thioxanthone (ITX, photo-sensitizer, PL Industries, PA) as the resin for making 3D printed Quake-style valves and pumps. ITX increases the absorption of the resin at the wavelengths where the spectra of ITX and Irgacure-819 overlap (~385 nm).[37] According to the Beer–Lambert law, an increase in resin absorption leads to a decrease in the characteristic penetration depth at the exposure wavelength (385 nm).[37] Thus, adding ITX to the resin allows us to fabricate the 25 μm-thick membranes and the 100 μm-deep flow-channels required for the Quake-style valve design. The resin is prepared by mixing Irgacure-819 and ITX with PEG-DA-258 with a mini vortexer and put in an oven at 70 °C for 30 min to complete the dissolution of ITX, which does not dissolve readily at room temperature. After the preparation process, the resin is stored at room temperature and kept in a polypropylene container wrapped in aluminum foil to prevent exposure to ambient light.

HEALTH WARNING: PEG-DA-258 resin (mixed with photoinitiator) is highly irritant and can cause severe burns and irritations. It should only be handled with gloves (double gloves for optimal protection) and in a very ventilated space (where no accumulations can occur) or inside a fume hood.

3D-printer

We use the DLP-SL (digital light processing - stereolithography) printer Asiga Pico2-HD (Sydney, Australia). This 3D-printer has an LED light source with UV wavelength 385 nm and LED power of 32.21 mW cm^{-2}. We chose Irgacure-819 as the photoinitiator because it has an absorbance peak close to 385 nm. The XY pixel resolution of the 3D printer's projector is 27 μm, and its minimum Z plane resolution is 10 μm. The maximum build size (printable area) of the print is 51.8 mm (X) × 29 mm (Y) × 75 mm (Z). 3D-printed devices can be printed successfully by setting an appropriate exposure time and calibrating the zero position of the build plate before starting the print. To assure all printed layers are fully reacted, the build plate should not lift too fast (<0.2 mm s^{-1}) after each layer is exposed.

The devices are printed on the silanized glass slide instead of being printed directly on the build plate to increase device transparency. Each glass slide is silanized with 3-(trimethoxysilyl)propyl methacrylate (TMSPMA, Sigma-Al-drich, MO). PEG-DA-258 is applied on the glass slide which is then placed on the build plate of the printer and exposed to UV light for ~3 s to secure it on the build plate.[34] After each print is completed, a small razor blade is used to remove the glass slide from the build plate and shave off any residue of cured PEG-DA-258 on the back side of the glass to provide a sharp and clean view of channels and valves under the microscope without any scratches imprinted on the device. The glass substrate also allows for easier removal of the print from the build plate since, in our case, the glass slide is slightly larger than the build plate. Removing the glass slide from the build plate minimizes the risk of damaging the printed device itself, and the flatness of glass slides helps the whole device sit on the microscope stage firmly and horizontally.

Valve/pump device fabrication

All devices are designed using the computer-aided design (CAD) program Autodesk Inventor. The connectors, which connect tubes and channels, can be either designed together with the valve in the same 3D CAD file or created separately and assembled with the valve design into a single 3D CAD file. The finished 3D CAD files are then converted to STL (stereolithography or standard triangle language) files for the 3D print software. The STL files are provided as ESI.†

The layer thickness of each layer is 25 μm and the exposure time of each layer was set to 160 ms. We chose 25 μm as the layer thickness because it is not too thick for the membrane to seal the valve seat with high pressure. Although the Z-axis resolution of the printer is 10 μm, we were not able to reproducibly make 10 μm-thick membranes that would resist both the fabrication process (the separation from the build plate tends to tear such thin membranes) and/or the operation. The print starts with a burn-in layer, which is the base of the printed device. We set the exposure time of the burn-in layer to 4.5 s. The membrane, which is located between the control and the flow channel, is the main component of the

valve structure (Fig. 1b). The valve is composed of a 25 μm-thick membrane placed between the extruded bowl-shape valve seat and the control chamber where the air pressure is applied. The shape of the membrane is defined by the deflectable, suspended region which is bounded by two parallel lines (1 mm) on two sides and two arcs on the other two sides (r = 0.5 mm). About 30 nL is displaced when the valve is closed. The height of the control channel and the flow channel are both 700 μm. The total volume of the liquid in the flow channel is 6.54 μL.

During printing, resin remains trapped inside the channel after the roof layers are printed, so the channel must be flushed and the unpolymerized resin must be completely removed before the device is exposed to ambient light to prevent clogged channels. Considering this, connectors play a key role during the valve fabrication process, in addition to their role as inlets and outlets during operation of the device, they provide a reliable fluidic path for the removal of unpolymerized resin. Flushing can be done either under ambient light or under dark/low-light conditions. If done under ambient light, the flushing must be done swiftly (<10 s, to prevent photopolymerization of the resin in the channel caused by the ambient light), otherwise flushing should be done under low-light conditions. As soon as the printing is finished, the build plate with the printed sample on it is covered with aluminum foil, taken into a dark room and soaked in deionized (DI) water for over 3 min. A syringe filled with DI water is used to flush out unpolymerized resin in both the flow and control channels of the device. Channels are flushed carefully several times and no vacuum is applied during the cleaning step in that the vacuum could inadvertently break the membrane.

Flow rate measurements

There are one flow channel and one control channel in the valve device. The inlet of the flow channel is connected to a bottle containing blue food coloring dye. The bottle is pressurized by a computer-controlled air pressure source (Elveflow OB1 MK3) to drive the dye into the flow channel. The fluid driving pressure is fixed at 0.2 psi. To observe the flow rate, the outlet of the flow channel is connected to the silicone tubing (0.79 mm I.D., Cole Parmer). As for the control channel part, the outlet is sealed with a plastic tube cap and the inlet is also connected to the air pressure source starting from 0 psi. The air pressure is increased in increments of 1 psi in the control channel until the valve closes such that movement of the front end of the fluid in the flow channel stops. Experiments were conducted in triplicate.

Current measurements to visualize the dynamic behavior of the valve

The flow channel of a microvalve (size: 1.2 mm-diam.) was filled with 0.1 M KCl solution as an electrolyte to provide conduction to a pair of electrodes inserted into the inlets. A constant voltage (5 V) was applied in the flow channel through connecting the inlet and outlet of the flow channel and a power supply with those electrodes (Fig. 4a). The experiment was started after assuring the current values shown on the oscilloscope are stable and there was no electrolysis observed during the test. The valve was opened and closed by applying 0 and 5 psi to the control channel, and the current changes were measured with an oscilloscope. Current changes as the valve was being closed and opened at different frequencies were recorded by the oscilloscope and plotted as a function of time to visualize the dynamic behavior of the valve. Experiments were conducted in triplicate.

Pump flow rate measurements

For these measurements, the flow channel of the pump device was filled with blue dye. The pumping sequence was initiated after assuring that the fluid was immobile in the flow channel. The head of the fluid was set to start in front of the valve closest to the outlet and pumped towards the outlet until the fluid head arrived at the outlet. There are a total of five states in the actuation sequence of the valves, with valves open and closed at different time periods. After finishing the first cycle of the sequence, the sequence was repeated as a loop in the last three steps. Pump flow rates were measured by recording videos for each condition and analyzing the liquid displacement in the channel with ImageJ and VLC media player (the time was recorded to the first decimal place).

Supplementary Material

Refer to Web version on PubMed Central for supplementary material.

Acknowledgements

We would like to acknowledge the National Cancer Institute (NCI), grant number R01CA181445 for partially supporting this work.

References

1. Harrison DJ, Fluri K, Seiler K, Fan Z, Effenhauser CS and Manz A, Science, 1993, 261, 895–897. [PubMed: 17783736]
2. Unger MA, Science, 2000, 288, 113–116. [PubMed: 10753110]
3. Grover WH, Skelley AM, Liu CN, Lagally ET and Mathies RA, Sens. Actuators, B, 2003, 89, 315–323.
4. Laser DJ and Santiago JG, J. Micromech. Microeng, 2004, 14, R35–R64.
5. Oh KW and Ahn CH, J. Micromech. Microeng, 2006, 16, R13–R39.
6. Au AK, Lai H, Utela BR and Folch A, Micromachines, 2011, 2, 179–220.
7. Kim J, Stockton AM, Jensen EC and Mathies RA, Lab Chip, 2016, 16, 812–819. [PubMed: 26864083]
8. Glick CC, Srimongkol MT, Schwartz AJ, Zhuang WS, Lin JC, Warren RH, Tekell DR, Satamalee PA and Lin L, Microsyst. Nanoeng, 2016, 2, 16063. [PubMed: 31057842]
9. Hansen CL, Sommer MOA and Quake SR, Proc. Natl. Acad. Sci. U. S. A, 2004, 101, 14431–14436. [PubMed: 15452343]
10. Li N, Hsu CH and Folch A, Electrophoresis, 2005, 26, 3758–3764. [PubMed: 16196107]
11. Hsu CH and Folch A, Appl. Phys. Lett, 2006, 89, 144102.
12. Frevert CW, Boggy G, Keenan TM and Folch A, Lab Chip, 2006, 6, 849. [PubMed: 16804588]
13. Cooksey GA, Sip CG and Folch A, Lab Chip, 2009, 9, 417–426. [PubMed: 19156291]
14. Zeng S, Li B, Su X, Qin J and Lin B, Lab Chip, 2009, 9, 1340. [PubMed: 19417898]
15. Hong JW, Studer V, Hang G, Anderson WF and Quake SR, Nat. Biotechnol, 2004, 22, 435–439. [PubMed: 15024389]
16. Ottesen EA, Hong JW, Quake SR and Leadbetter JR, Science, 2006, 314, 1464–1467. [PubMed: 17138901]
17. Maerkl SJ and Quake SR, Science, 2007, 315, 233–237. [PubMed: 17218526]
18. Gómez-Sjöberg R, Leyrat AA, Pirone DM, Chen CS and Quake SR, Anal. Chem, 2007, 79, 8557–8563. [PubMed: 17953452]
19. Gu W, Zhu X, Futai N, Cho BS and Takayama S, Proc. Natl. Acad. Sci. U. S. A, 2004, 101, 15861–15866. [PubMed: 15514025]

20. Lam EW, Cooksey GA, Finlayson BA and Folch A, Appl. Phys. Lett, 2006, 89, 164105.
21. Hsu CH and Folch A, Appl. Phys. Lett, 2005, 86, 023508.
22. Thorsen T, Science, 2002, 298, 580–584. [PubMed: 12351675]
23. Volpetti F, Garcia-Cordero J and Maerkl SJ, PLoS One, 2015, 10, e0117744. [PubMed: 25680117]
24. Au AK, Bhattacharjee N, Horowitz LF, Chang TC and Folch A, Lab Chip, 2015, 15, 1934–1941. [PubMed: 25738695]
25. Gong H, Bickham BP, Woolley AT and Nordin GP, Lab Chip, 2017, 17, 2899–2909. [PubMed: 28726927]
26. Beauchamp MJ, Nordin GP and Woolley AT, Anal. Bioanal. Chem, 2017, 409, 4311–4319. [PubMed: 28612085]
27. Lee W, Kwon D, Choi W, Jung GY, Au AK, Folch A and Jeon S, Sci. Rep, 2015, 5, 7717. [PubMed: 25578942]
28. Kitson PJ, Rosnes MH, Sans V, Dragone V and Cronin L, Lab Chip, 2012, 12, 3267. [PubMed: 22875258]
29. Keating SJ, Gariboldi MI, Patrick WG, Sharma S, Kong DS and Oxman N, PLoS One, 2016, 11, e0160624. [PubMed: 27525809]
30. Rogers CI, Qaderi K, Woolley AT and Nordin GP, Biomicrofluidics, 2015, 9, 016501. [PubMed: 25610517]
31. Bhattacharjee N, Urrios A, Kang S and Folch A, Lab Chip, 2016, 16, 1720–1742. [PubMed: 27101171]
32. Waheed S, Cabot JM, Macdonald NP, Lewis T, Guijt RM, Paull B and Breadmore MC, Lab Chip, 2016, 16, 1993–2013. [PubMed: 27146365]
33. Gong H, Woolley AT and Nordin GP, Lab Chip, 2016, 16, 2450–2458. [PubMed: 27242064]
34. Urrios A, Parra-Cabrera C, Bhattacharjee N, Gonzalez-Suarez AM, Rigat-Brugarolas LG, Nallapatti U, Samitier J, DeForest CA, Posas F, Garcia-Cordero JL and Folch A, Lab Chip, 2016, 16, 2287–2294. [PubMed: 27217203]
35. Rogers CI, Oxborrow JB, Anderson RR, Tsai LF, Nordin GP and Woolley AT, Sens. Actuators, B, 2014, 191, 438–444.
36. Armani D, Liu C and Aluru N, Micro Electro Mech. Syst. 1999. MEMS ‘99; IEEE Int. Conf, 1999, pp. 222–227.
37. Kuo AP, Bhattacharjee N and Folch A, Micro TAS, 2017.
38. Chou HP, Unger MA and Quake SR, Biomed. Microdevices, 2001, 3, 323–330.
39. Wang C-H and Lee G-B, J. Micromech. Microeng, 2006, 16, 341–348.
40. Lai H and Folch A, Lab Chip, 2011, 11, 336–342. [PubMed: 20957288]

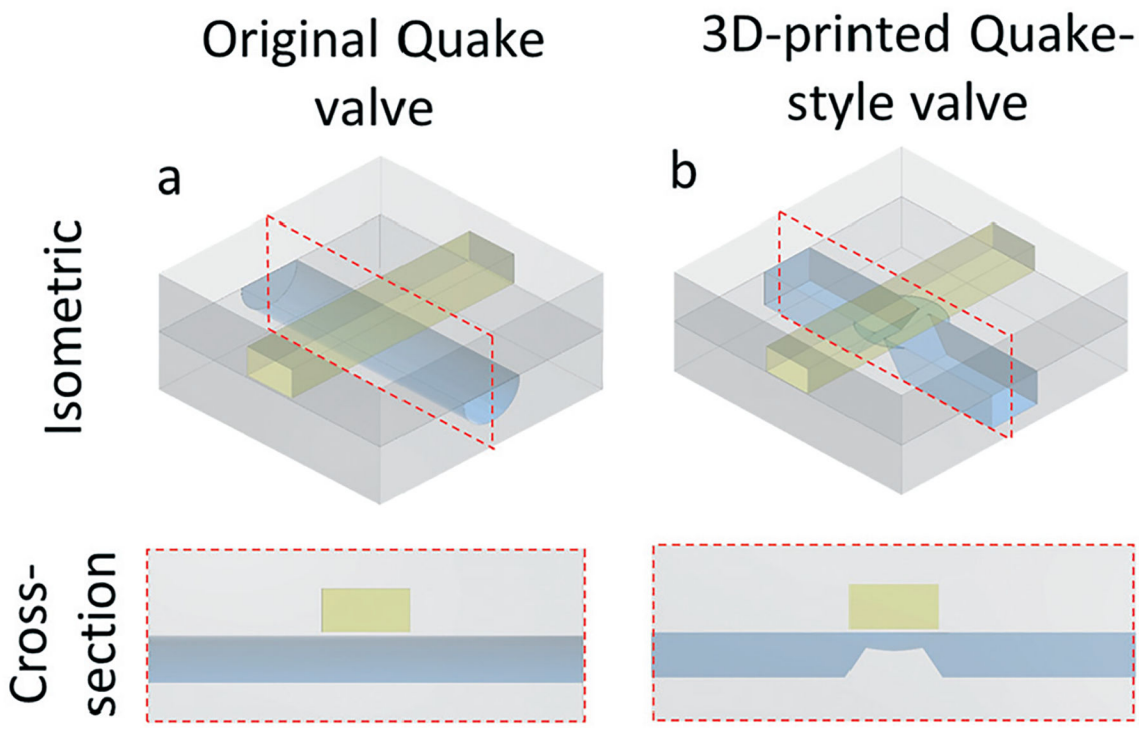

Fig. 1.

Isometric and cross-section views of the (a) original Quake valve design, with a semi-cylindrical seat, and (b) our 3D-printed Quake-style valve design, with a hemispherical cap seat. The cross-section views are captured from the red-dashed rectangles shown in the isometric views. The STL files of both valve designs are available in ESI.†

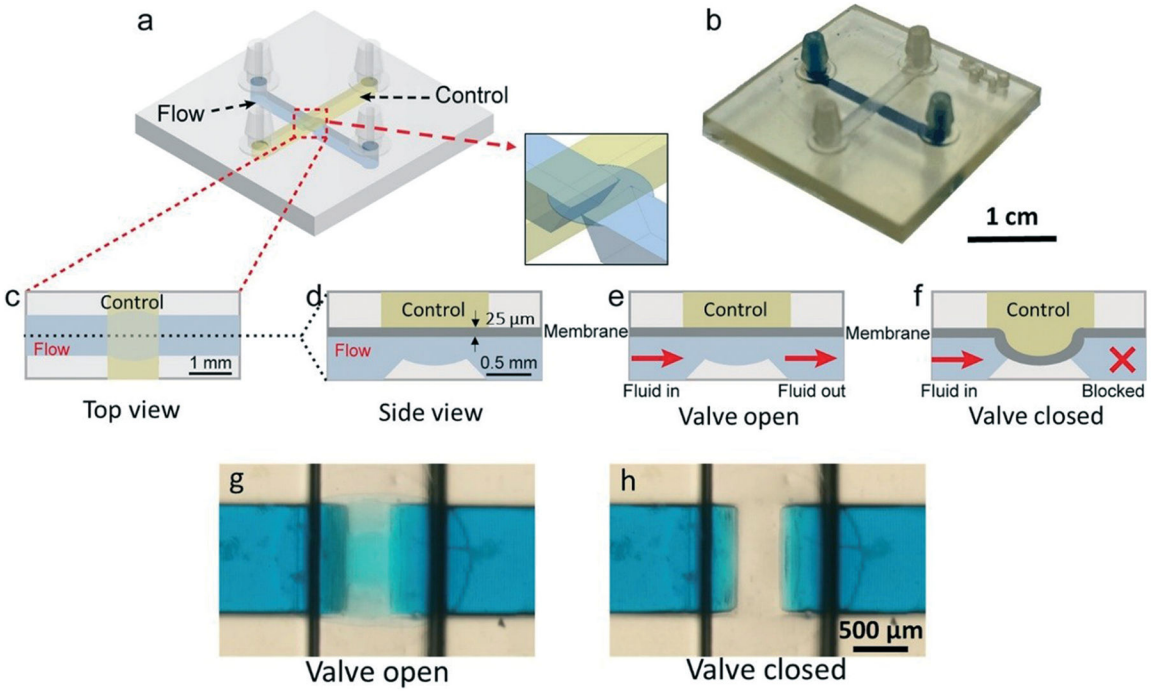

Fig. 2.

CAD design and the working principle of the 3D-printed "Quake-Style" valve, featuring a 1200 μm-diam. membrane. (a) Isometric diagram, showing the 3D structure of the device. (b) Photographs of a 3D-printed Quake-style valve device with no external connections. For visualization purposes, the flow channel is filled with blue dye while the control channel, filled with air, appears transparent. (c–f) 2D schematics showing the operation of the valve, with blue and yellow identifying the flow channel and the control channel, respectively. (c) Top-view schematic of the valve. (d–f) Side-view schematics showing (d) dimensions of the valve, (e) the valve in its open state, and (f) the valve in its closed state. (g) Micrograph of the valve in its open state (0 psi) applied to the control channel. (h) Micrograph of the valve in its closed state (5 psi).

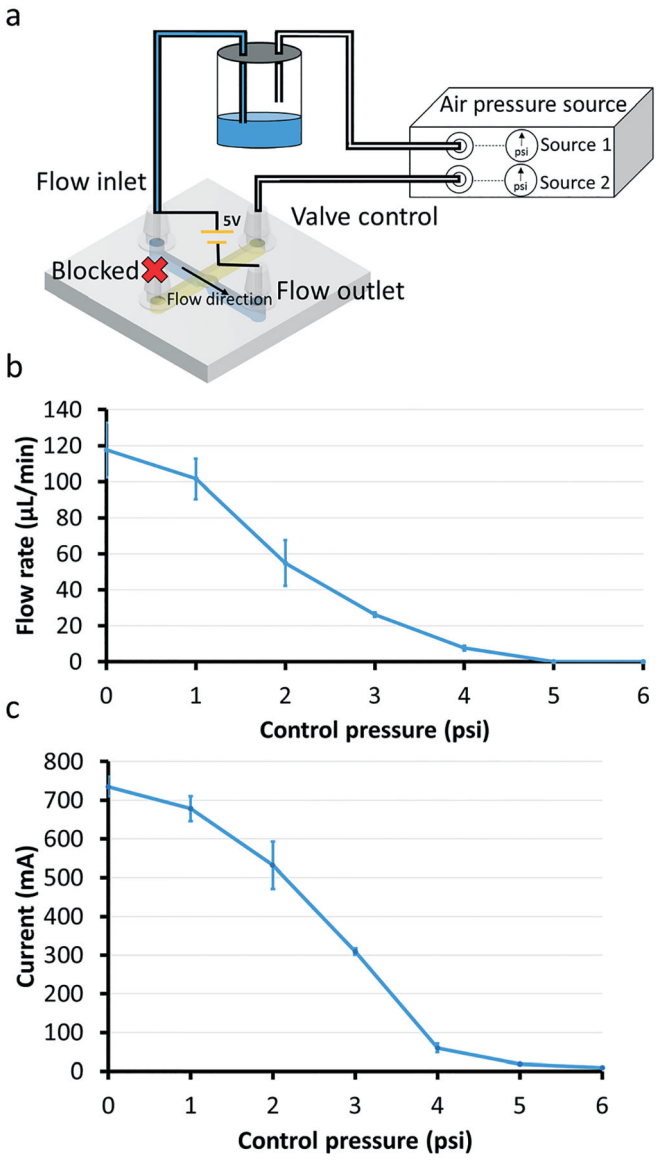

Fig. 3.

Flow rate measurements with 1200 μm-diam. valves. (a) Device setup for flow rate experiments. We used a digital pressure source (Elveflow OB1 MK3 system) to control the pressure applied to the control channel. One of the digital pressure outputs is connected to a liquid bottle in order to siphon the fluid out of the bottle and into the flow channel (shown as blue in the valve's schematic diagram). The end of the control channel that is not connected to the bottle is kept blocked. Flow rates vary when different pressures are applied to the control channel. (b) Graph of the flow rate as a function of pressure applied to the Quake-style valve through the control channel. The pressure driving the flow is 0.2 psi for all data points ($n = 3$). Note that the fluid in the flow channel can be fully stopped when the applied pressure is above 5 psi. The error bars represent standard error of the mean. (c) Graph of the current through the flow channel as a function of the control pressures applied to the valve. A voltage of 5 V is applied to the flow channel filled with a saline solution (0.1 M KCl). The

current detection setup is shown in Fig. 4a. As the control pressure increases, the current detected by the oscilloscope decreases. The current is ~4 mA when the applied pressure in the control channel is 6 psi. The pressure driving the flow is 0.2 psi for all data points (n = 3). The error bars represent standard error of the mean.

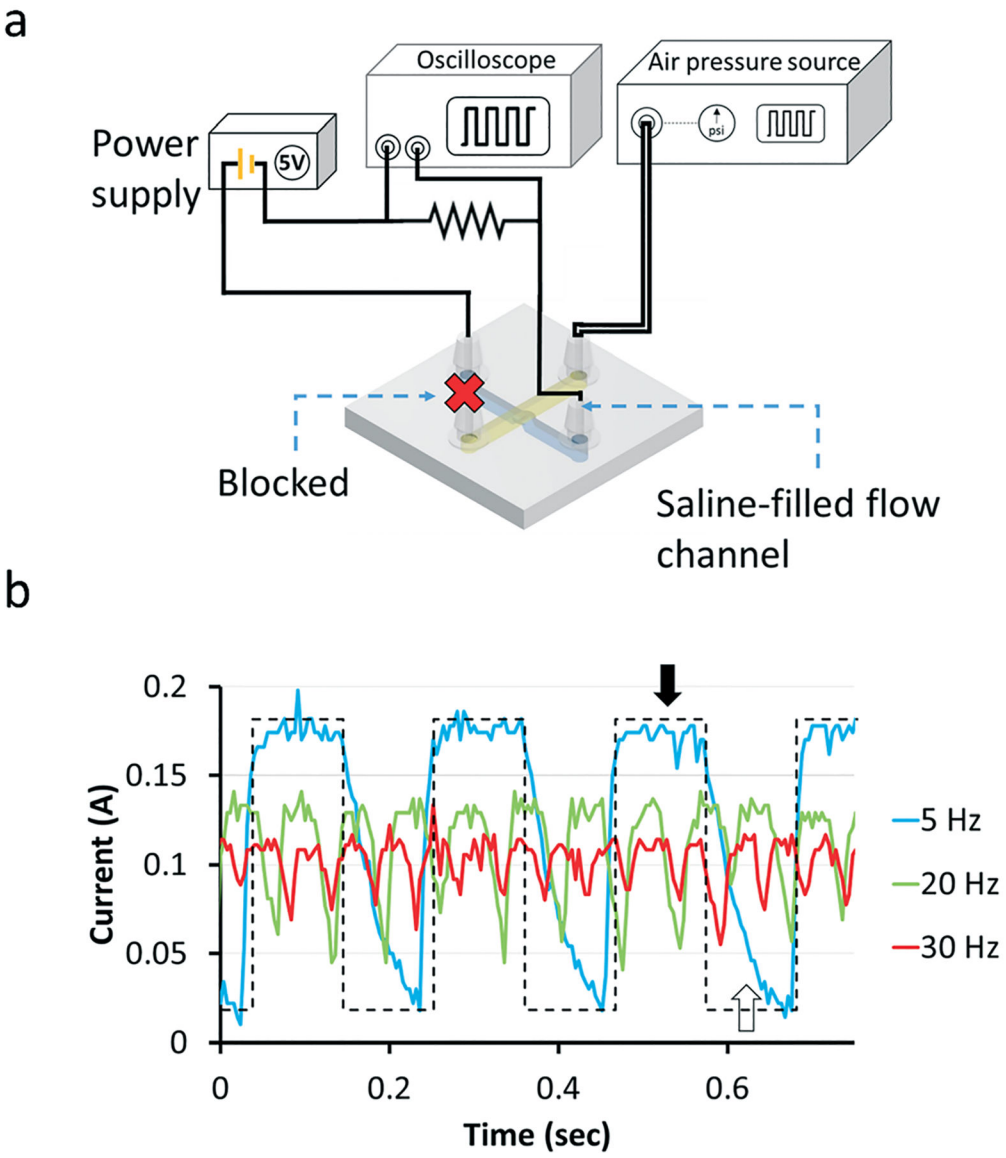

Fig. 4.

Measurement of valve dynamics with a 1200 μm-diam. valve. (a) The flow channel is filled with 0.1 M KCl solution. The inlet and outlet of the flow channel (colored with blue) are connected to an electric circuit, one end of the flow channel is connected to the power supply and the other end is connected to an oscilloscope. The voltage of the power supply is set to 5 V. A pressure of 5 psi is applied to the control channel (colored with yellow). (b) Voltage changes during the valve opening and closing states at three valve actuation frequencies (5, 20 and 30 Hz). The black and white arrows show the fully open and fully closed states, respectively. The dashed line shows the ideal current change at 5 Hz assuming the valve responds infinitely fast to the pressure changes.

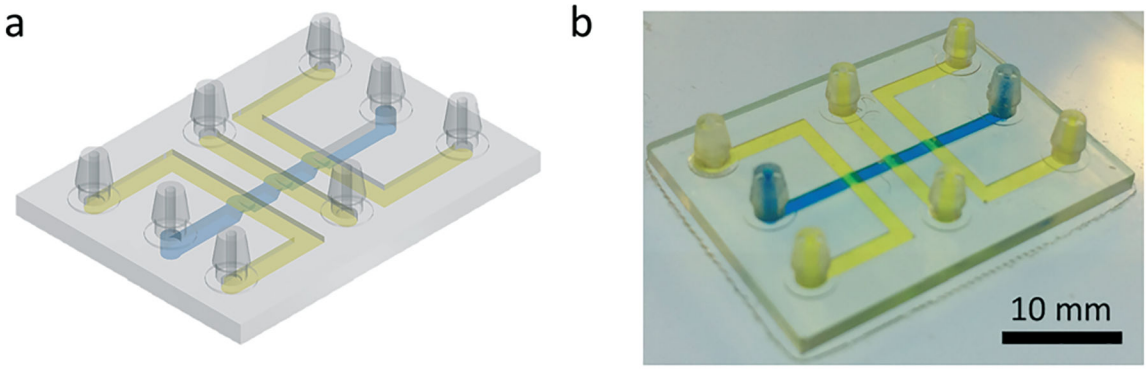

Fig. 5.

3D-printed Quake-style pump featuring 1200 μm-diam. valves. (a) Isometric view of the CAD design of the Quake-style pump. (b) Isometric view of the 3D-printed Quake-style pump. The flow channel and control channels are shown in blue and yellow, respectively. The STL file of the micropump design is available in ESI.†

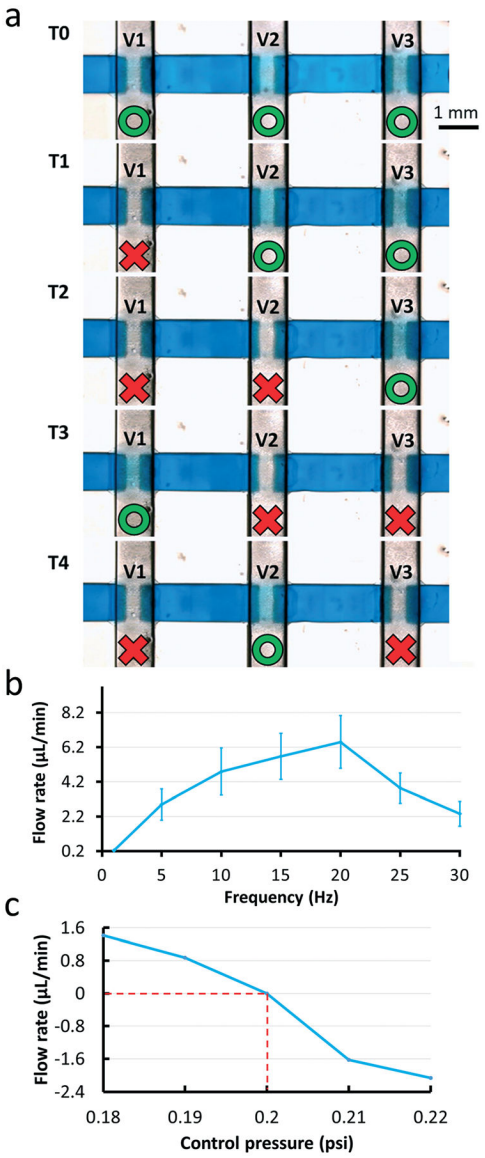

Fig. 6.

(a) The valve actuation sequence used to control a Quake-style pump with 1200 μm-diam. valves. In the first state (T0), all valves are open. The states denoted from T0 to T4 show each state of the 5-phase actuation. Each valve n (V_n) is closed in the T_n state and in the T_{n+1} state. After finishing the first round, from T0 to T4 states, the valve closing cycle repeats between the T2 state and T4 state; the red color represents the state of valve closed state and the green represents the valve open state. (b) Graph of the relationship between pump rates and pump actuation frequencies. The valve closing pressure is fixed at 7 psi. The pump has the highest flow rate when the pump actuation frequency is 20 Hz. Experiments were conducted in triplicate. (c) Graph of pumping flow rates *versus* the head pressure that the 3D-printed Quake-style pump can work against when the control pressure is 14 psi with 20 Hz pump actuation frequency. When a pressure of 0.2 psi is applied at the outlet of the flow channel, the fluid stalls. The fluid moves forward (positive flow rates) when the head

pressure is less than 0.2 psi and backward (negative flow rates) when the head pressure is greater than 0.2 psi.

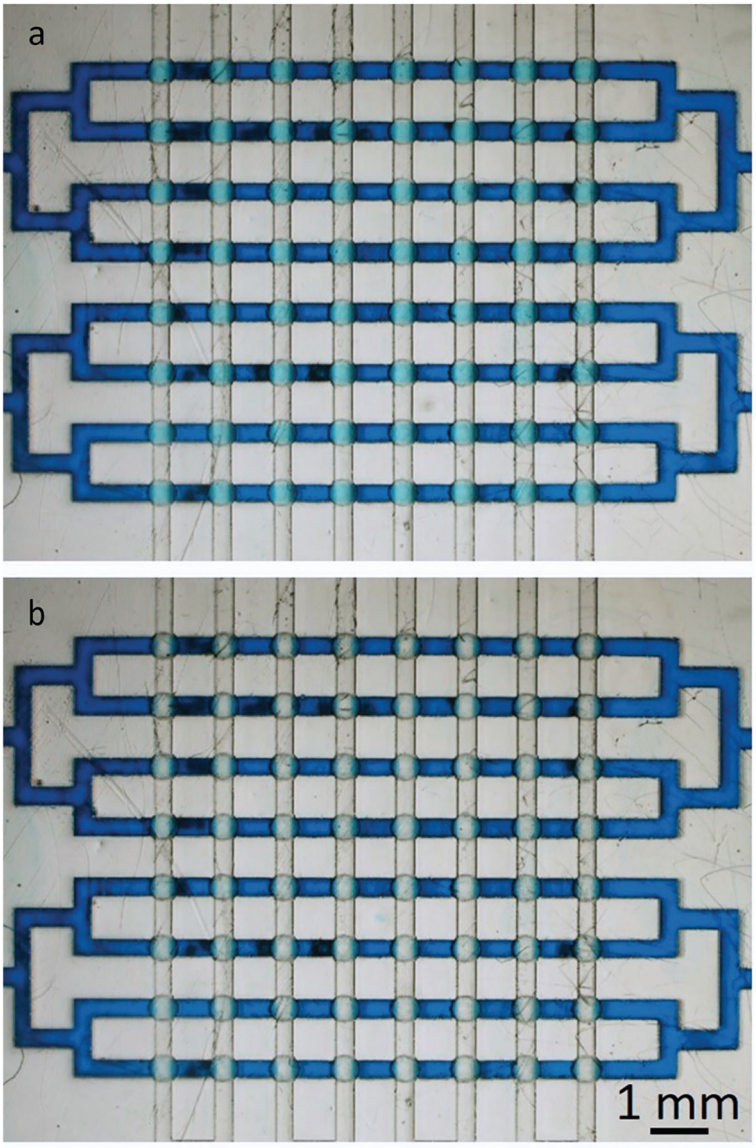

Fig. 7.

The 3D-printed Quake-style microvalve array of 64 valves (500 μm-diam. valves). All the flow channels share one common inlet and outlet and all the control channels also share one common inlet and outlet. (a) All valves are open without applying any pressure to the control channels. (b) All the valves are closed by applying 3 psi to the control channels.